

Numerical Analysis to Investigate the Impact of Skirt Geometric Parameters on Secondary Piston Movement in a Single-cylinder Diesel Engine

Brahim Menacer^{1*}, Sunny Narayan², Mostefa Bouchetara³, Tawfiq Khatir⁴, Pedro Daniel Urbina Coronado²

¹ Laboratoire des Systèmes Complexe, Ecole Supérieure en Génie Electrique et Energétique, Chemin Vicinal 9, 31000 Oran, Algeria

² Escuela de Ingeniera y Ciencias, Tecnológico de Monterrey, Ave. Eugenio Garza Sada 2501, 64849 Monterrey, Mexico

³ Laboratory of Gas Combustion and Environment, Department of Mechanical Engineering, University of Sciences and the Technology of Oran, 31000 Oran, P.O.B. 1505, Algeria

⁴ Artificial Intelligence Laboratory for Mechanical and Civil Structures, and Soil, Institute of Technology, University Center of Naama, 45000 Naama, P.O.B. 66, Algeria

* Corresponding author, e-mail: menacer_brahim@esgee.dz

Received: 22 April 2023, Accepted: 12 October 2023, Published online: 18 October 2023

Abstract

Currently, modern internal combustion engines are receiving great attention due to their efficiency, particularly in response to the increasing limits imposed by environmental and emission legislation. Sound emissions of internal combustion engines are mainly caused by three sources of noise: combustion, mechanical and aerodynamic flow. The secondary motion of the piston plays a crucial role in the analysis of performance, noise, vibration and reliability of internal combustion engine (ICE). In the presented article, a mathematical simulation model has been developed by using of the GT-Suite software to study the rotational and lateral motion of the piston (called secondary motion) as well as the piston slap in ICE. This model takes into account the effect of variation in the major geometric parameters of the skirt design, such as the piston pin offset (P.P.O) and the length of the skirt. Furthermore, a combined model that accounts for the interplay between the secondary dynamics of the piston and the dynamic fluid lubrication has been developed. This model utilizes a mixed lubrication approach for the purpose of simulation. The results of this simulation have demonstrated that the variations in length of the skirt and the P.P.O have a considerable effect on piston secondary motion and tribological performances, and that the lateral motion of the piston is significantly influenced by the piston side force, which plays a crucial role in this behavior.

Keywords

noise, vibrations, piston tilt, piston eccentricity, diesel engine, GT-Suite software

1 Introduction

In the internal combustion engine (ICE), the piston is subjected to two distinct types of movement. The first type is the primary motion, which consists of a back-and-forth motion between two points top dead center (TDC) and bottom dead center (BDC) [1]. This motion converts the pressure generated by the fuel combustion into mechanical work that drives the engine. The second type is the secondary motion, which refers to the piston's motion in lateral and rotational directions [2]. This motion can have significant consequences on the engine's performance, vibration and lubrication. Indeed, this secondary motion can increase the friction and wear of components such as cylinder walls, piston rings, and bearings [3]. There are numerous research

studies in literature that are dedicated to examining the secondary motion of pistons, specifically concerning the effectiveness, emissions, and longevity of engines, such as [4, 5].

Lu et al. [6] examined the effects of various factors such as connecting rod inertia, piston skirt profiles, piston offset, and thermal deformation on lubrication performance and piston secondary motion. The results revealed that these factors have a significant impact on both lubrication performance and piston secondary motion.

The objective of the study conducted by Guo et al. [2] was to examine the impact of secondary piston motion combined with clearances joints on the performance and durability of internal combustion engines. The results

indicated that secondary motion increased loads on the piston rings and cylinder walls, thus affecting the durability and performance of the engine.

Forero et al. [7] proposed a mathematical model that incorporates the deformation of the piston skirt and considers the effects of clearances in the connecting rod bearings in order to enhance the accuracy of estimations for the secondary movement of the piston. The findings of the study reveal that throughout the combustion cycle, the piston experiences six changes in direction, accompanied by lateral and angular velocities reaching up to 0.13 m/s and 4 rad/s, respectively. Furthermore, the hydrodynamic forces acting on the connecting rod bearings increase by approximately 500 N as a result of these motions.

Tan et al. [8] devised a numerical model with three degrees of freedom to examine the secondary motion of the piston. The outcomes indicate that when the damping coefficient and stiffness are low, the piston exhibits bouncing behavior against the cylinder liner, leading to vibrations in the engine block. However, as the damping coefficient of the piston increases, these vibrations diminish. Moreover, when the stiffness of the piston segment is augmented, the amplitude of piston bounce and engine block vibration decreases.

Bhavi et al. [9] reported an experimental study that examines the impact of piston connecting rod offset on the reduction of noise and vibrations caused by piston slap. In this study, three values of connecting rod offset (0.2, 0.3, and 0.4 mm) and experiments were carried out on an operating ICE to obtain the frequency spectrum of noise and vibrations. Additionally, noise level curves in terms of dB(A) were generated through these experiments. The purpose of these experiments was to investigate the frequency components of the engine noise and vibrations, and to assess the overall noise levels in terms of dB(A) for various operating conditions, including different piston motions, bearing clearances, and combustion dynamics. The results showed that a piston connecting rod offset of 0.3 mm had a positive impact on stress values and on the reduction of noise intensity on the internal combustion engine studied.

In this study, a numerical simulation model is developed to investigate the variation with crank angle of the piston tilting, the top and bottom piston eccentricities, piston thrust side force and the hydrodynamic performances in mixed lubrication. The GT-Suite simulation software was utilized for this purpose. The dynamic equations associated with the piston's secondary motion were solved, and the impacts of different skirt designs were analyzed.

2 Governing equation of the secondary motion of the piston

Fig. 1 illustrates the dynamic movement of the piston. Under the pressure exerted by the gas on the upper part of the skirt, the piston moves along the cylinder liner, generating a hydrodynamic oil force around the skirt, represented by F_h , and a moment M_h . The translation and rotation movements of the piston are called top (et) and bottom (eb) eccentricities of the skirt. In this paper, the following assumptions have been taken into account during the modeling [8, 10]:

- only three degrees of freedom of piston motion are taken into account, namely the primary piston motion (one degree of freedom) and the secondary piston motion (two degrees of freedom);
- the oil used in the power cylinder unit is considered a Newtonian and incompressible fluid;
- assuming the absence of cavitation and full immersion of the piston skirt in oil, the governing equation for the secondary motion of the piston is formulated without considering thermal and elastic deformation of the piston skirt and liner;
- the oil film thickness is considered thin compared to the lateral size of the piston [11].

Noise and vibrations are generated when the secondary motion of the piston, caused by various eccentricities, causes it to collide with the cylinder liner [12]. The distance

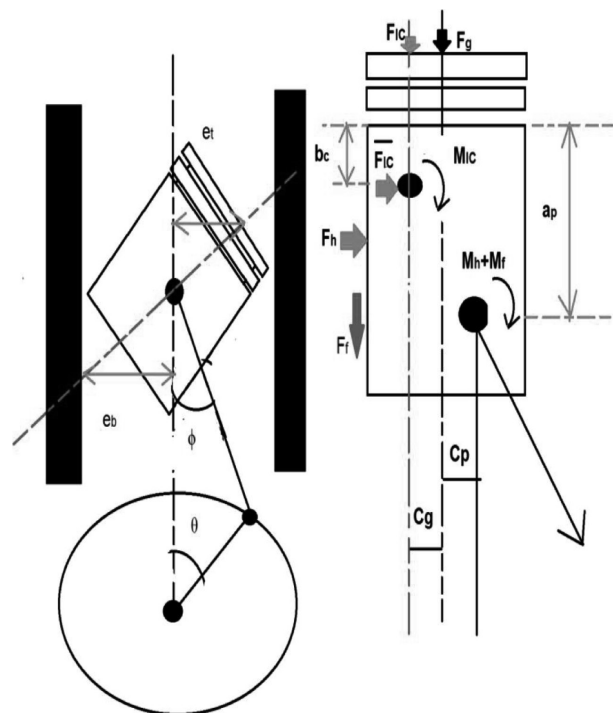


Fig. 1 Piston dynamic model

traveled by the piston along the cylinder liner, denoted as Z , can be expressed as a function of several parameters, such as the piston pin radius r , the connecting rod length l , the piston pin offset C_p , and the tilt angle ϕ as follows in Eq. (1) [13]:

$$Z = -r_p \cos(\theta) - (l^2 - B_s^2) + \sqrt{(l + r_p)^2 - C_p^2}, \quad (1)$$

where $B_s = r_p \sin(\theta) + C_p$.

By applying the first and second derivative of the previously mentioned equation (Eq. (1)), the piston velocity and acceleration are given by [14]:

$$\frac{\delta Z}{\delta t} = \left[\frac{B_p}{\sqrt{l^2 - B_p^2}} \cos \phi + \sin \phi \right] r \omega, \quad (2)$$

$$\begin{aligned} \frac{\delta^2 Z}{\delta t^2} = & r \omega \times \cos \phi + \frac{(r \omega B_p \cos \phi)^2}{\sqrt{l^2 - B_p^2}} \\ & + \frac{r \omega^2 (r \cos \phi \cos \phi - B_p \cos \phi)}{\sqrt{l^2 - B_p^2}}. \end{aligned} \quad (3)$$

The inertia force acting on the X-axis, denoted F_{IC} , can be formulated as follows in Eq. (4) [15]:

$$F_{IC} = - \begin{pmatrix} m_{pist} + m_{pin} \\ + m_{sl} \end{pmatrix} \begin{bmatrix} r_p \omega \cos \theta + \frac{(r_p \omega B_s \cos \theta)^2}{\sqrt{l^2 - B_s^2}} \\ r_p \omega^2 \begin{pmatrix} r_p \cos^2 \theta \\ -B_s \cos \theta \end{pmatrix} \\ + \frac{r_p \omega^2}{\sqrt{l^2 - B_s^2}} \end{bmatrix}. \quad (4)$$

The force exerted by the gases on the top of the piston, represented by F_g , can be calculated based on the cylinder gas pressure, denoted P_g , and the diameter of the piston, D , as follows in Eq. (5) [16]:

$$F_g = P_g \times \pi \times \frac{D^2}{4}. \quad (5)$$

In addition to the inertia force acting along the X-axis, the piston is also subjected to a force along the Y-axis, which can be expressed in terms of the upper and lower eccentricities (et , eb) as follows in Eq. (6) [17]:

$$F'_{IC} = (m_{pist} + m_{pin} + m_c) \left[\frac{\delta^2 et}{\delta t^2} - \frac{b_c}{L} \left(\frac{\delta^2 et}{\delta t^2} - \frac{\delta^2 eb}{\delta t^2} \right) \right]. \quad (6)$$

The displacement (y), velocity (v), and acceleration (a) of the piston along the Y-axis can be defined as follows in Eqs. (7) to (9) [18]:

$$y = et + \frac{b_c}{L} (et - eb), \quad (7)$$

$$v = \frac{b_c}{L} \left(\frac{\delta eb}{\delta t} \right) + \frac{L - b_c}{L} \left(\frac{\delta et}{\delta t} \right), \quad (8)$$

$$a = \frac{\delta^2 et}{\delta t^2} - \frac{b_c}{L} \left(\frac{\delta^2 et}{\delta t^2} - \frac{\delta^2 eb}{\delta t^2} \right). \quad (9)$$

When the piston moves inside the liner, the friction between the liner and the skirt creates a shear force (τ) in the oil film. This force can be formulated as follows in Eq. (10) [19]:

$$\tau = \mu \frac{U}{h}, \quad (10)$$

where U is the skirt velocity in the axial direction, h is the minimum film thickness and μ is the oil dynamic viscosity.

Using the shear stress, it is possible to calculate the friction force between the skirt and the liner (F_f) as well as the resulting moment around the piston (M_f) as follows in Eqs. (11) and (12) [18, 20]:

$$F_f = R \iint \tau(x, \theta) dx d\theta, \quad (11)$$

$$M_f = R \iint \tau(x, \theta) (R \cos \theta - C_p) dx d\theta. \quad (12)$$

The force of the oil film (F_h) and its moment around the wrist pin (M_h) generated by the nonlinear pressure distribution $p(x, \theta)$ can be expressed as follows in Eqs. (13) and (14) [21]:

$$F_h = R \iint [p(x, \theta)] \cos \theta dx d\theta, \quad (13)$$

$$M_h = R \iint [p(x, \theta)] (a_p - x) \cos \theta dx d\theta. \quad (14)$$

When the piston changes direction, it undergoes a tilt at an angle (γ). The moment of rotation around the wrist pin can be defined as follows in Eq. (15):

$$M_{IC} = - \frac{I_{pist}}{L} \left(\frac{\delta^2 et}{\delta t^2} - \frac{\delta^2 eb}{\delta t^2} \right). \quad (15)$$

In addition, different forces and moments balance equations are employed to describe the system dynamics of the piston's secondary motion, can be formulated as follows in Eqs. (16) to (18) [22]:

$$F_g + F_{IC} + F_f + F_L \cos \varphi = 0, \quad (16)$$

$$F_h + F'_{IC} + F_L \sin \varphi = 0, \quad (17)$$

$$M_h + M_{IC} + F'_{IC}(a_p - b_c) + F_g C_p - F_{IC} C_g + M_f = 0. \quad (18)$$

The numerical model can be formulated in matrix form as follows in Eq. (19) [23, 24]:

$$\begin{bmatrix} m_{pist} \left(1 - \frac{b_c}{L}\right) & m_{pist} \left(\frac{b_c}{L}\right) \\ +m_{pin} \left(1 - \frac{a_p}{L}\right) & +m_{pin} \left(\frac{a_p}{L}\right) \\ m_{pist} \left(1 - \frac{a_p}{L}\right)(b_c - a_p) & m_{pist} \left(\frac{a_p}{L}\right)(b_c - a_p) \\ +\left(\frac{I_{pist}}{L}\right) & -\left(\frac{I_{pist}}{L}\right) \end{bmatrix} \begin{bmatrix} e''t \\ e''b \end{bmatrix} = \begin{bmatrix} F_h - (F_{IC} + F_g + F_f) \tan \phi \\ M_h + M_f + F_g C_p - F_{IC} C_g + F'_{IC}(a_p - b_c) \end{bmatrix}. \quad (19)$$

Due to the non-linear behavior of forces and moments acting on the piston, the pressure distribution in the lubrication film is not uniform. As a result, the Reynolds hydrodynamic lubrication model, as referenced in [3], is frequently utilized to describe the system dynamics. The model is formulated as follows in Eq. (20):

$$\begin{aligned} & \frac{\partial}{\partial x} \left(\phi_x h^3 \frac{\partial p}{\partial x} \right) + \frac{\partial}{\partial y} \left(\phi_y h^3 \frac{\partial p}{\partial y} \right) \\ & = 6\mu U \left(\frac{\partial h}{\partial y} + \sigma \frac{\partial \phi_s}{\partial y} \right) + 12\mu \frac{\partial h}{\partial t}. \end{aligned} \quad (20)$$

Equation (21) describes the thickness of the lubrication film (h) [3]:

$$h = C_{pc} + et \cos \theta + \frac{y}{L_{ps}} \cos \theta (eb - et) + d. \quad (21)$$

In the Reynolds hydrodynamic lubrication model, the clearance between the piston skirt and the cylinder liner is denoted by " C_{pc} ", and " d " represents the elastic deformation of the piston induced by the pressure of the lubrication film.

3 Results and discussion

The findings presented in this study pertain to a single-cylinder, four-stroke direct injection diesel engine operating at 2000 revolutions per minute (rpm) under full load conditions. The key parameters utilized in the simulation are summarized in Table 1.

To assess the dependability of the mathematical model devised in this research, a comparative analysis is performed between the gas pressure findings derived from the mathematical model and those obtained from experimental tests [25], as depicted in Fig. 2. The comparison reveals a strong correspondence between the numerical and experimental gas pressure values, indicating a significant correlation between the two sets of data, with an estimated error of about 3% between the two.

Table 1 Engine data

Parameter	Value	Units
Bore	119	mm
Stroke	100	mm
Length of connecting rod	300	mm
Connecting-rod mass	1900	g
Crank radius	31.5	mm
Crank mass	1260	g
Length of piston skirt	70/75/80	mm
Liner material	Al	–
Skirt surface roughness	0.4	–
Skirt-cylinder friction coefficient	0.12	–
Elasticity modulus of the cylinder liner	75	GPa
Cylinder liner poisson's ratio	0.33	–
Piston Material	Al	–
Piston mass	1200	g
Elasticity modulus of the piston	75	GPa
Piston poisson's ratio	0.33	–
Density of the used oil	881.5	kg/m ³
Dynamic viscosity of the lubricant	0.008736	Pa·s

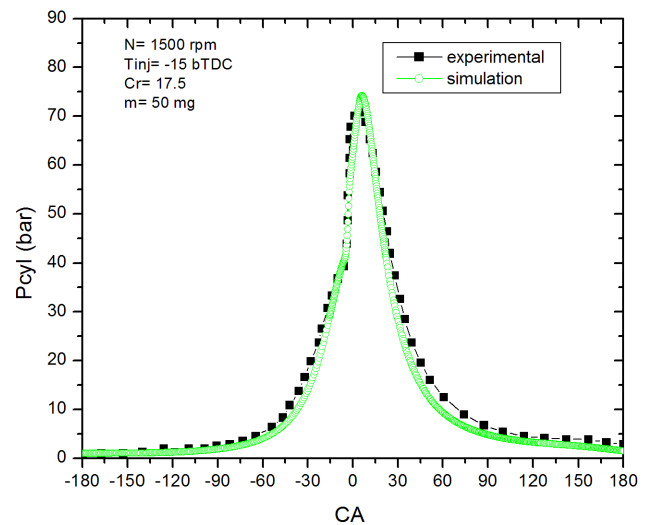


Fig. 2 In-cylinder simulated and experimental gas pressure as a function of crank angle

3.1 Effect of the piston-skirt length

The study of piston dynamics is strongly influenced by the length of the piston skirt. Fig. 3 shows the influence of the skirt length on the secondary movement of the piston (namely, lateral and angular displacement). The variations in eccentricities range from -1.5 to 2.0 microns for a skirt length of 70 mm and is from -3.0 to 2.5 for a skirt length of 75 mm. Fig. 3 shows that the eccentricity and tilt of the piston increase proportionally to the length of the piston skirt, both for the top and bottom skirts. The most significant variations in skirt eccentricity are observed when the gas forces acting on it are maximal, particularly at crank angle positions of 0° during the power stroke.

Fig. 4 illustrates the impact of varying piston skirt length on the resultant piston side thrust force. This force undergoes five changes in direction during a complete engine cycle, implying the possibility of five occurrences of lateral contact between the piston skirt and the cylinder liner. The highest variation in force is observed at a crank angle of 0° during the power stroke, which corresponds to a maximal cylinder pressure.

Fig. 5 illustrates the influence of the length of the piston skirt on its tribological properties. Specifically, Fig. 5(a) shows the evolution of the minimum oil film thickness, while Fig. 5(b) highlights the frictional power losses over an engine cycle. The results show that the minimum oil film thickness decreases as the length of the piston skirt is increased, whether it is for major or minor thrust.

The hydrodynamic frictional power losses exhibit a sinusoidal curve. Furthermore, the energy dissipation due to frictional power consumption resulting from the shear stress of the lubrication oil exhibits a relatively uniform pattern. The hydrodynamic frictional power loss reaches its maximum value when the piston is at TDC and a value of zero when the piston is at BDC, whether it is for major or minor thrust.

3.2 Effect of the piston pin offset

The engine piston can be placed on either the thrust or anti-thrust side of the cylinder liner. However, both positions can pose a problem. To reduce lateral movement of the skirt, the offset must be towards the thrust side, while to minimize wear, it should be oriented towards the anti-thrust side [6]. In the presented results, positive values of the piston pin offset distance indicate that the offset is oriented towards the anti-thrust side, while negative values indicate that it is turned towards the thrust side.

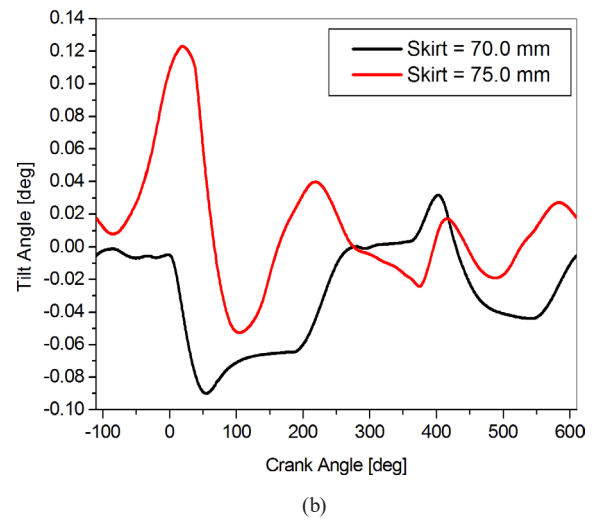
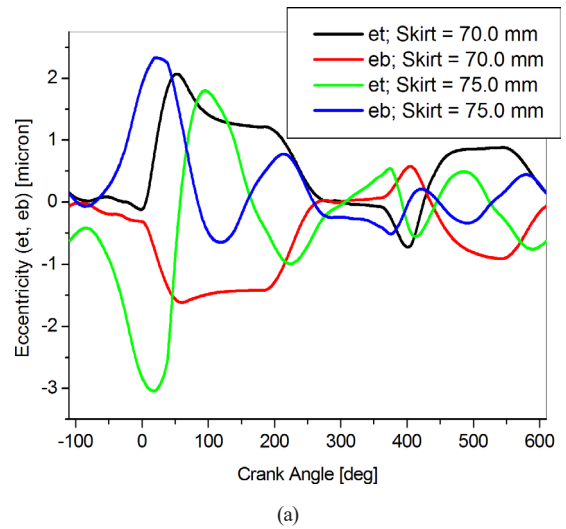


Fig. 3 Effect of piston-skirt length on the piston secondary motion; (a) Lateral displacement (variations in top and bottom eccentricity of skirt); (b) Angular displacement (variations in tilting angle of skirt)

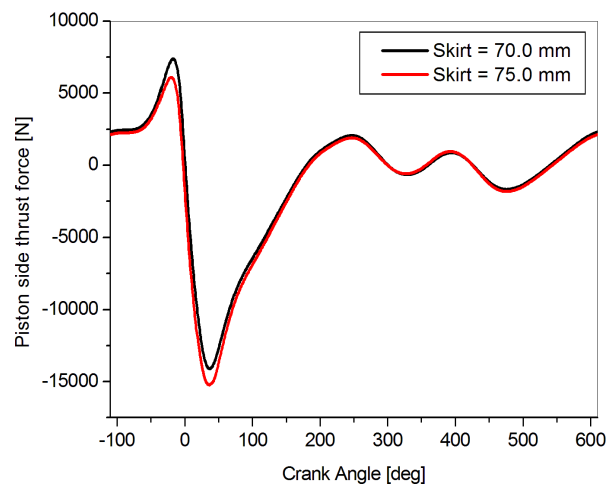
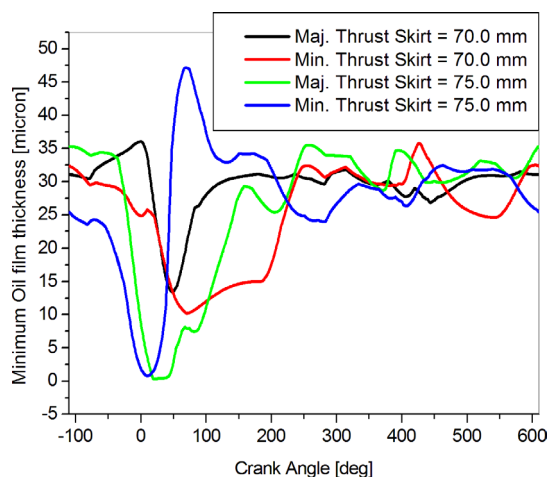
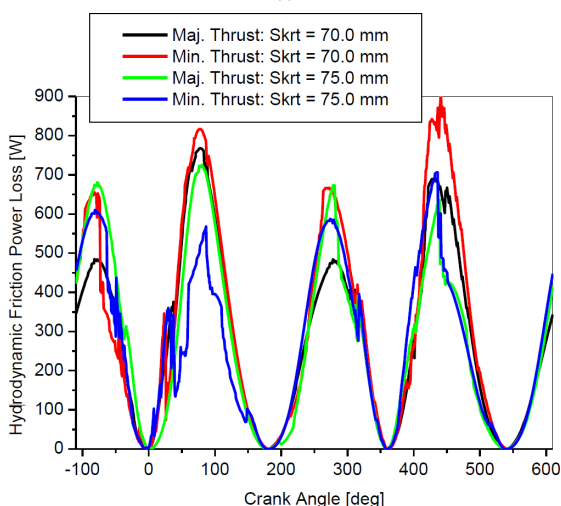


Fig. 4 Length of the piston skirt effect on the magnitude of the piston side thrust force



(a)

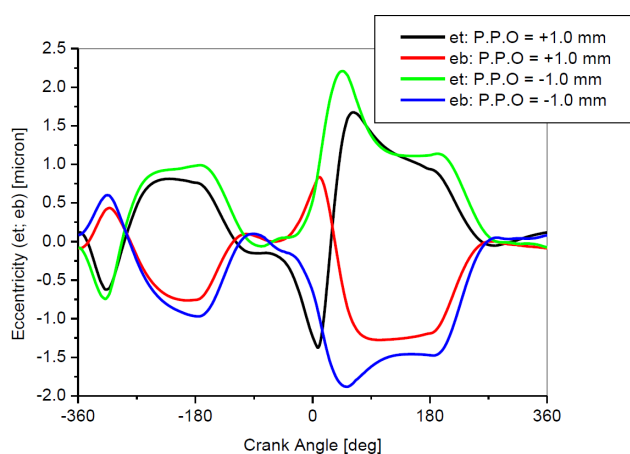


(b)

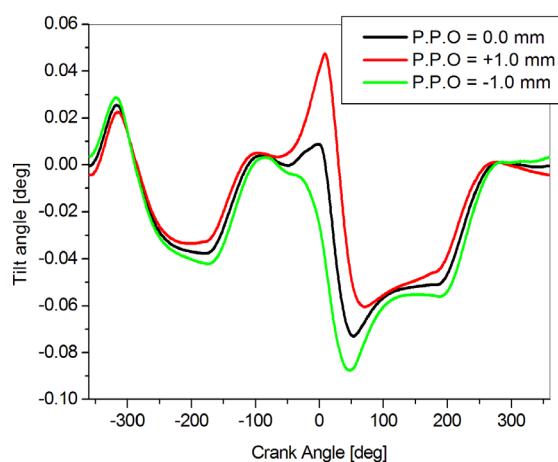
Fig. 5 Effect of the piston-skirt length on the tribological characteristics; (a) Oil film thickness; (b) Hydrodynamic friction power loss

Fig. 6(a) and (b) show, respectively, the comparisons of the eccentricity of the top and bottom of the piston skirt and the tilt angle of the piston using three different offset values of -1 mm (thrust side), 0 mm (central location), and $+1$ mm (anti-thrust side). It noticed that the top and the bottom eccentricity increases if the piston pin offset moved from the thrust side (piston pin offset (P.P.O) = -1) to the anti-thrust side (P.P.O = $+1$). The most variations of top and bottom eccentricity are observed at crank angle positions of 0° during the power stroke. The adjustment of the piston pin has a significant impact on the piston tilting angle during the compression and the working stroke. The most critical position is during the reversal of the piston at the TDC.

Fig. 7 shows the effect of the piston pin offset on the piston side thrust force. The highest variation in force is observed at a crank angle of 0° during the power stroke, which corresponds to a maximal cylinder pressure. The piston pin offset does not have a remarkable impact on the piston side thrust force.



(a)



(b)

Fig. 6 Effect of piston pin offset on the piston secondary motion; (a) Lateral displacement (variations in top and bottom eccentricity of skirt); (b) Angular displacement (variations in tilting angle of skirt)

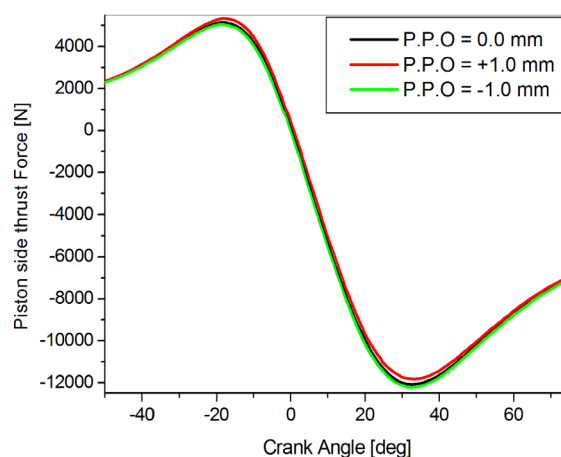


Fig. 7 Effect of the piston pin offset on the piston side thrust force

Fig. 8(a) and (b) illustrate respectively the influence of the piston pin offset on the minimum oil film thickness and on the frictional power losses during an engine cycle. The results show that the minimum oil film thickness decreases if the piston pin offset moved from the thrust side

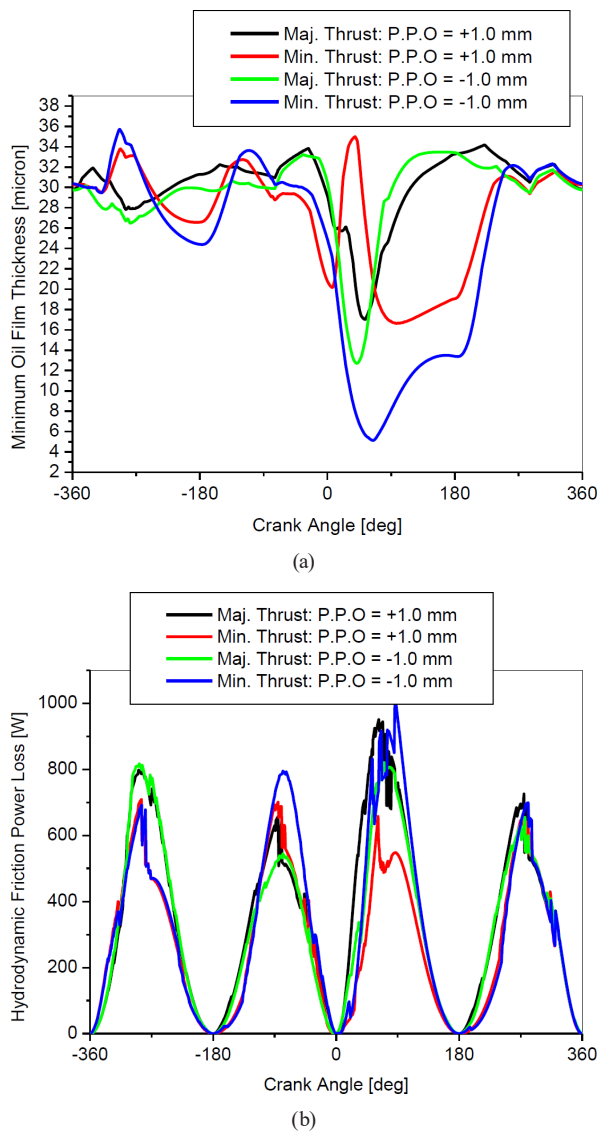


Fig. 8 Effect of the piston pin offset on the tribological characteristics; (a) Oil film thickness; (b) Hydrodynamic friction power loss

(P.P.O = -1) to the anti-thrust side (P.P.O = +1), whether it is for major or minor thrust. The hydrodynamic friction power losses demonstrate a sinusoidal pattern. The hydrodynamic friction power loss is at its highest when the piston is at

TDC, and reaches zero when the piston is at BDC, regardless of whether it is for a major or minor thrust.

4 Conclusion

In this research article, a numerical simulation model is developed using GT-Suite software to investigate the secondary motion of the piston. The study focuses on analyzing the effects of skirt length and piston pin offset on piston secondary motion, piston skirt side force, and tribological performance. Based on the research findings, the following conclusions can be drawn:

- Augmenting the length of the piston skirt results in greater lateral displacement and an increase in the piston tilt angle, which consequently raises the lateral acceleration of the piston. As a result, the impact forces experienced by the piston are amplified in magnitude.
- The piston secondary motion and side force increase with increasing of piston pin offset from -1.0 mm (thrust side) to +1.0 mm (anti thrust side). This variation can impact in fluctuations in the oil film thickness and hydrodynamic power loss.

Certainly, this mathematical model can be utilized to simulate the effects of other design parameters, such as piston mass and lubricant viscosity, on the dynamics of the piston and lubrication. For future research, there are plans to incorporate considerations for the profile and deformation of the piston skirt, and conduct a detailed investigation into their influence on the tribological performance of the piston and cylinder liner.

Acknowledgement

This study was performed under the framework of "Project Impact Socio-Economique" Contract N° 362 funded by the General Directorate of Algerian Scientific Research (DGRSDT).

References

- [1] Gamble, R. J., Priest, M., Chittenden, R. J., Taylor, C. M. "Preliminary Study of the Influence of Piston Secondary Motion on Piston Ring Tribology", Tribology Series, pp. 679–691, 2000. [https://doi.org/10.1016/s0167-8922\(00\)80171-6](https://doi.org/10.1016/s0167-8922(00)80171-6)
- [2] Guo, J., Randall, R. B., Borghesani, P., Smith, W. A., Haneef, M. D., Peng, Z. "A study on the effects of piston secondary motion in conjunction with clearance joints", Mechanism and Machine Theory, 149, 103824, 2020. <https://doi.org/10.1016/j.mechmachtheory.2020.103824>
- [3] Menacer, B., Bouchetara, M. "Parametric Analysis of the Effect of Engine Speed and Load on the Hydrodynamic Performance of the Lubricant in Diesel Engine", Periodica Polytechnica Mechanical Engineering, 64(4), pp. 299–306, 2020. <https://doi.org/10.3311/PPme.15725>
- [4] Buzzoni, M., Mucchi, E., Dalpiaz, G. "A CWT-based methodology for piston slap experimental characterization", Mechanical Systems and Signal Processing, 86, pp. 16–28, 2017. <https://doi.org/10.1016/j.ymssp.2016.10.005>

- [5] Kirner, C., Halbhuber, J., Uhlig, B., Oliva, A., Graf, S., Wachtmeister, G. "Experimental and simulative research advances in the piston assembly of an internal combustion engine", *Tribology International*, 99, pp. 159–168, 2016.
<https://doi.org/10.1016/j.triboint.2016.03.005>
- [6] Lu, Y., Li, S., Wang, P., Liu, C., Zhang, Y., Müller, N. "The Analysis of Secondary Motion and Lubrication Performance of Piston considering the Piston Skirt Profile", *Shock and Vibration*, 2018, 3240469, 2018.
<https://doi.org/10.1155/2018/3240469>
- [7] Forero, J. D., Ochoa, G. V., Alvarado, W. P. "Study of the Piston Secondary Movement on the Tribological Performance of a Single Cylinder Low-Displacement Diesel Engine", *Lubricants*, 8(11), 97, 2020.
<https://doi.org/10.3390/lubricants8110097>
- [8] Tan, Y.-C., Ripin, Z. M. "Analysis of piston secondary motion", *Journal of Sound and Vibration*, 332(20), pp. 5162–5176, 2013.
<https://doi.org/10.1016/j.jsv.2013.04.042>
- [9] Bhavi, I., Kuppast, V. V., Chillal, D. D. "Experimental Investigation of Influence of Piston Pin-Offset on Reduction of Piston Slap Noise", *Journal of Failure Analysis and Prevention*, 21(4), pp. 1195–1202, 2021.
<https://doi.org/10.1007/s11668-021-01193-9>
- [10] Zhao, B., Dai, X.-D., Zhang, Z.-N., Xie, Y.-B. "A new numerical method for piston dynamics and lubrication analysis", *Tribology International*, 94, pp. 395–408, 2016.
<https://doi.org/10.1016/j.triboint.2015.09.037>
- [11] Dolatabadi, N., Littlefair, B., De la Cruz, M., Theodossiadis, S., Rothberg, S. J., Rahnejat, H. "A transient tribodynamic approach for the calculation of internal combustion engine piston slap noise", *Journal of Sound and Vibration*, 352, pp. 192–209, 2015.
<https://doi.org/10.1016/j.jsv.2015.04.014>
- [12] Flores, P., Ambrósio, J., Claro, J. C. P., Lankarani, H. M. "Translational Joints With Clearance in Rigid Multibody Systems", *Journal of Computational and Nonlinear Dynamics*, 3(1), 011007, 2008.
<https://doi.org/10.1115/1.2802113>
- [13] Narayan S., Gupta, V. "Numerical Analysis of Secondary Motion of Piston Skirt in Engines", *International Journal of Acoustics and Vibration*, 23(4), pp. 557–565, 2018.
<https://doi.org/10.20855/ijav.2018.23.41513>
- [14] McFadden, P. D., Turnbull, S. R. "Dynamic analysis of piston secondary motion in an internal combustion engine under non-lubricated and fully flooded lubricated conditions", *Proceedings of the Institution of Mechanical Engineers, Part C: Journal of Mechanical Engineering Science*, 225(11), pp. 2575–2585, 2011.
<https://doi.org/10.1177/0954406211408674>
- [15] Kim, T. J. "Numerical analysis of the piston secondary dynamics in reciprocating compressors", *KSME International Journal*, 17(3), pp. 350–356, 2003.
<https://doi.org/10.1007/BF02984361>
- [16] Offner, G., Herbst, H. M., Priebsch, H. H. "A methodology to simulate piston secondary movement under lubricated contact conditions", *SAE Technical Paper*, USA, 2001-01-0565, 2001.
<https://doi.org/10.4271/2001-01-0565>
- [17] Haddad, S. D., Tjan, K.-T. "An analytical study of offset piston and crankshaft designs and the effect of oil film on piston slap excitation in a diesel engine", *Mechanism and Machine Theory*, 30(2), pp. 271–284, 1995.
[https://doi.org/10.1016/0094-114X\(94\)00035-J](https://doi.org/10.1016/0094-114X(94)00035-J)
- [18] Mansouri, S. H., Wong, V. W. "Effects of piston design parameters on piston secondary motion and skirt - liner friction", *Proceedings of the Institution of Mechanical Engineers, Part J: Journal of Engineering Tribology*, 219(6), pp. 435–449, 2005.
<https://doi.org/10.1243/135065005X34026>
- [19] Gamma technologies "GT-Suite software, (7.4)", [computer program] Available at: <https://www.gtisoft.com/gt-suite/> [Accessed: 21 April 2023]
- [20] Gunelsu, O., Akalin, O. "Development of a piston secondary motion model for skirt friction analysis", In: *ASME 2012 Internal Combustion Engine Division Fall Technical Conference*, Vancouver, BC, Canada, pp. 963–970, 2012. ISBN 978-0-7918-5509-6
<https://doi.org/10.1115/ICEF2012-92166>
- [21] Fang, C., Meng, X., Xie, Y. "A piston tribodynamic model with deterministic consideration of skirt surface grooves", *Tribology International*, 110, pp. 232–251, 2017.
<https://doi.org/10.1016/j.triboint.2017.02.026>
- [22] Vu, T. D., Durville, D., Davies, P. "Finite element simulation of the mechanical behavior of synthetic braided ropes and validation on a tensile test", *International Journal of Solids and Structures*, 58, pp. 106–116, 2015.
<https://doi.org/10.1016/j.ijsolstr.2014.12.022>
- [23] Dursunkaya, Z., Keribar, R., Ganapathy, V. "A model of piston secondary motion and elasto-hydrodynamic skirt lubrication", *Journal of Tribology*, 116(4), pp. 777–785, 1994.
<https://doi.org/10.1115/1.2927332>
- [24] Guzzomi, A. L., Hesterman, D. C., Stone, B. J. "Variable inertia effects of an engine including piston friction and a crank or gudgeon pin offset", *Proceedings of the Institution of Mechanical Engineers, Part D: Journal of Automobile Engineering*, 222(3), pp. 397–414, 2008.
<https://doi.org/10.1243/09544070JAUTO590>
- [25] Narayan, S. "Correlation between cylinder pressure and noise emissions from diesel engines", *Journal of KONES*, 22(1), pp. 243–254, 2015.
<https://doi.org/10.5604/12314005.1161775>